Available online at www.sciencedirect.com

ScienceDirect

Advances in Space Research 56 (2015) 2542–2551

ADVANCES IN SPACE RESEARCH (a COSPAR publication)

www.elsevier.com/locate/asr

Statistical analysis of TEC perturbations over a low latitude region during 2009–2013 ascending solar activity phase

Geoffrey Andima [a,*], Edward Jurua [a], Emirant Bertillas Amabayo [a,b], John Bosco Habarulema [c]

[a] Department of Physics, Mbarara University of Science and Technology, P O Box 1410, Mbarara, Uganda
[b] South African National Space Agency (SANSA) Space Science, P O Box 32, Hermanus 7200, South Africa
[c] Department of Physics, Busitema University, P O Box 236, Tororo, Uganda

Received 15 May 2015; received in revised form 12 September 2015; accepted 14 September 2015
Available online 21 September 2015

Abstract

Total Electron Content (TEC) perturbations are manifestations of ionospheric irregularities which induce fluctuations in the amplitude and phase of trans-ionospheric radio signals. TEC data derived from Global Positioning System (GPS) receivers at Mbarara (Geogra. −0.60°N, 30.74°E and Geomag. −10.22°N, 102.36°E) and Entebbe (Geogra. 0.04°N, 32.44°E and Geomag. −9.53°N, 104.10°E) from 2009 to 2013 were used to study TEC perturbations over the low latitude region of Uganda. The results show that the frequency of occurrence of TEC perturbations of >4 TECU increased steadily from 2009 to 2013. TEC perturbations with amplitude <4 TECU occurred at all times. The likelihood of TEC perturbations exceeding 6 TECU was higher during the equinoxes than during the solstices in most of the years. Comparison of TEC perturbations with 10.7 cm solar radio flux (F10.7) data showed a weak positive correlation with this solar proxy. Wavelet analysis performed on the TEC perturbations revealed wave-like oscillations with periods typical of Traveling Ionospheric Disturbances (TID). These wave-like structures (WLS) dominated from 13:00 to 19:00 LT for most of the years analyzed. Though the WLS were observed to increase with solar activity, no seasonal pattern was recorded in their occurrence.

Keywords: Total Electron Content; Low-latitude TEC perturbations; Traveling Ionospheric Disturbances

1. Introduction

The equatorial and low latitude ionospheric electron density distribution, is governed by electrodynamic processes at the magnetic equator (Balan et al., 1997). As a result of these processes, unique features such as Equatorial Ionization Anomaly (EIA), Equatorial Electro Jet (EEJ), etc are exhibited by the low latitude ionosphere. Martyn (1947) explained these features in terms of the interaction between the mutually perpendicular electric and Earth's magnetic fields. During daytime, the E region electric field is eastward, and causes a large plasma fountain by $E \times B$ drift at the magnetic equator. The raised plasma diffuses due to pressure gradient and gravity forces towards higher latitudes to form crests at about 15° on either side of the magnetic equator. Just before the electric field turns westwards at night, the eastward electric field is enhanced by a local dynamo that develops at the bottom of the F layer, often referred to as Pre Reversal Enhancement (PRE). The PRE raises the plasma further resulting in irregular plasma density distributions. The up and down plasma drifts are also responsible for current systems in the upper atmosphere. One such a current system is the EEJ which flows in the region close to the magnetic equator. The EEJ induces a local magnetic field in a narrow

* Corresponding author.
E-mail address: geoffrey.andima@gmail.com (G. Andima).

http://dx.doi.org/10.1016/j.asr.2015.09.021
0273-1177/

band along the magnetic equator, and this magnetic field perturbs the magnetic field due to the Earth. Fluctuations in the ionospheric electric field influences the magnitude of the EEJ, which in turn determines the day to day ionospheric plasma dynamics over the low latitude region.

The equatorial electrodynamics, and the low latitude ionosphere are modulated by global factors such as solar activity and geomagnetic storms. Solar activity variations affect the E region electric fields, thus influencing the strength of the EIA as well as the magnitude of EEJ. Galav et al. (2010) observed a contraction in the crest of the EIA during a declining solar activity period. Magnetospheric electric fields during storms may also suppress or enhance the fountain effect at the geomagnetic equator. Mendillo (2006) reviewed the different mechanisms through which storm time electric fields may reach low latitudes and impart on the low latitude ionospheric dynamics. In addition to these global factors, oscillations in EIA (Chen, 1992) and pre reversal electric fields (Abdu et al., 2006) have been observed. These oscillations were attributed to Gravity Waves (GW). The GW interact with plasma to produce the well known Traveling Ionospheric Disturbances (TID) (Hernández-Pajares et al., 2006). MacDougall et al. (2013) explained the possible mechanisms for these interactions, while Fritts and Alexander (2003) reviewed the dynamics of GW in the middle atmosphere. TID are commonly classified into large and medium scales. According to Hunsucker (1982), Large Scale TID (LSTID) have phase speeds of >300 m s^{-1}, and periods in the range 1–3 h while Medium Scale TID (MSTID) have phase speeds ranging from 100 to 300 m s^{-1} and periods ranging from 10 min to 1 h.

The above factors make the low latitude ionosphere variable and therefore characterizing the ionosphere is important for applications such as geodesy, satellite based navigation, and radio communication. Significant Total Electron Content (TEC) perturbations affect systems that use Earth-space environment such as satellite telephones, satellite televisions, and remote sensing of the Earth using satellites. Many researchers have studied low latitude TEC under different conditions such as disturbed (Habarulema et al., 2013b; D'ujanga et al., 2013), low solar activity (Liu et al., 2012; Galav et al., 2010), ascending phase of solar activity (Olwendo et al., 2012a,b; D'ujanga et al., 2013) and during high solar activities (Klausner et al., 2009). Despite these various investigations over the low latitude regions, not much has been reported on the degree of TEC perturbations especially over the Ugandan region. Quantifying the amplitude of these TEC perturbations is essential in predicting the hourly and daily variability of the ionosphere.

The purpose of this paper is therefore to statistically present the extent of TEC perturbations over the low latitude region using Global Position System (GPS) TEC. To investigate the contribution of the solar flux to ionospheric perturbations, the TEC deviations were compared with 10.7 cm solar radio flux (F10.7) data. In the last section of this paper, wave-like structures (WLS) in the TEC perturbations were identified and characterized.

2. Data and analysis

The data used in this study were downloaded from GPS receivers installed at Mbarara (station code MBAR) and Entebbe (station code EBBE). The coordinates of the GPS receivers used and the available data from 2009 to 2013 are given in Table 1. We collected Receiver INdependent EXchange (RINEX) files from the GPS receivers and then obtained the integral number of electrons along the line of sight (LOS), called slant TEC (sTEC) using GPS_TEC algorithm developed at Boston college (Seemala and Valladares, 2011). The GPS_TEC algorithm calculates the sTEC in TEC Units (TECU), with 1 TECU equivalent to 10^{16} electrons per 1 m^2 using the equation

$$\text{sTEC} = \int_R^S N_e dl, \tag{1}$$

where N_e is the number of electrons per m^3, R and S are the receiver and satellite positions respectively, and dl the element of length along the LOS. The algorithm corrects for the biases in the sTEC and then applies the thin shell mapping function and epoch-by-epoch averaging to calculate the vertical TEC (vTEC) for satellites with elevation angles above 20°. In this study, we averaged the vTEC from different satellites over a period of 30 s. This was to minimize calibration errors from individual satellites. Possible errors due to multipath contamination of the calculated vTEC and those due to the thin shell approximation used in the slant-to-vertical mapping procedure were significantly reduced by using only data from satellites with elevation angles greater than 30°.

To study ionospheric perturbations, we calculated the monthly medians for all the months in each year under investigation. The monthly medians were then used as the background diurnal TEC and these were subtracted from the daily TEC values. Important to note is that, 2012 data were not analyzed in this study due to data paucity.

2.1. Procedure for identifying the wave-like structures

TEC perturbations due to TID are quite easy to identify in a simple varying TEC data (Katamzi et al., 2012). However, the high noise levels and poor GPS receiver alignment presented an extra challenge in identifying TID. A possible method could have been the Statistical Angle-of-arrival and Doppler Method (SADM) (Afraimovich et al., 1998). The SADM is limited in that it requires an interferometry array of three GPS receivers in an assumed x–y plane. Such an array was not available over the region studied. We therefore adopted three filtering techniques to characterize WLS that occur in the TEC perturbations. First we minimized the noise levels by applying adaptive Savitzky–Golay filter to the observed diurnal TEC. This filter when applied to equally spaced data values $f_i = f(t_i)$,

Table 1
Coordinates of the GPS receiver stations and the data availability for the years analyzed.

Station code	Geogra. coordinates		Geomag. coordinates		Data availability (days)				
	Longitude (°E)	Latitude (°N)	Longitude (°E)	Latitude (°N)	2009	2010	2011	2012	2013
EBBE	32.44	0.04	104.10	−9.53	301	178	313	47	143
MBAR	30.74	−0.60	102.36	−10.22	362	176	146	119	333

where $i = n_L, \ldots, n_R$ and $t_i = t_o + i\Delta t$, replaces each data value f_i in a window of width $[n_L n_R]$ by a linear combination h_i of the values within that window.

$$h_i = \sum_{n=n_L}^{n_R} C_n f_i + n \tag{2}$$

where n_L and n_R are the number of data points to the left and right of the central point f_i respectively. The coefficients C_n were determined by a least square fit of a polynomial of order 6 to a window of $n_R = n_L = 60$. A detailed description of Savitzky–Golay filter can be found in Luo et al. (2005). Plots of the filtered TEC were generated and WLS in the TEC were identified.

Different methods have been used to detrend TEC to identify TID in TEC perturbations. For example polynomial fitting (Katamzi et al., 2012; Habarulema et al., 2013a) and moving average (Hernández-Pajares et al., 2006) have all performed quite well. Without introducing artificial periodicities in the TEC data, we applied a least square polynomial fit of degree 6 to the vTEC. The polynomial was evaluated and then the values subtracted from the diurnal TEC of the days that showed the WLS. Since the purpose was to characterize WLS in TEC perturbations, our third filter involved isolating periods of interest. We used the continuous wavelet transform to extract periods (10 min to 3 h) with notable TID. The complex Morlet wavelet (cmor) was used as the mother wavelet. It is a complex exponential function modified by a Gaussian envelope expressed as

$$\Psi(x) = \frac{1}{\sqrt{\pi f_b}} e^{2i\pi f_c x} e^{-\frac{x^2}{f_b}}, \tag{3}$$

where f_b is the bandwidth parameter and f_c is the center frequency (Misiti, 2005). In particular we used MATLAB complex Morlet wavelet cmor4-1.5 ($f_b = 4$ and $f_c = 1.5$) to determine the dominant periods of the WLS.

3. Results and discussions

3.1. TEC perturbations

To characterize the low latitude ionosphere, TEC perturbations from 2009 to 2013 were analyzed. The TEC perturbations were arrived at by subtracting the monthly median TEC values from the daily TEC and this yielded TEC perturbations at every 30 s. The overall variation of the TEC perturbations observed at EBBE and MBAR GPS stations in 2009–2013 are shown in Fig. 1. The white spaces in the plots in Fig. 1 were due to missing data. Fig. 1 shows that significant TEC perturbations occurred mainly between 09:00 and 00:00 LT (LT = UT + 3 h). TEC perturbations of larger amplitude were fewer in 2009 than those observed in 2013. The equinoctial months of March–April and September–October had larger TEC perturbations than the rest of the months in 2009 (Fig. 1(c) and (d)). These observations show diurnal and seasonal variations in TEC perturbations over the low latitude region which are consistent with results of similar studies (e.g., Galav et al. (2010), Amabayo et al. (2014), Liu et al. (2012), Olwendo et al. (2012a), and Adewale et al. (2012)) over the low latitude region. To investigate the contribution of solar flux variations to ionospheric variability, the TEC perturbations in Fig. 1 were statistically analyzed and the results are discussed in the following subsections.

3.1.1. Diurnal variation of TEC perturbations

For the diurnal variation, only hourly averages of TEC perturbations greater than 2 TECU were used. This threshold was arrived at by first determining probabilities of days having TEC perturbations of amplitude 0.5 TECU, 1.0 TECU, 1.5 TECU, 2.0 TECU, etc. TEC perturbations of less than 2 TECU were almost a daily occurrence and therefore were not used in this analysis. Furthermore, TEC perturbations from 00:00 to 06:00 LT were generally small and were also not analyzed. The TEC perturbations were divided into intervals of $2 \leqslant \Delta\text{TEC} < 4$, $4 \leqslant \Delta\text{TEC} < 6$, $6 \leqslant \Delta\text{TEC} < 8$ and $\Delta\text{TEC} \geqslant 8$TECU. To compare the TEC perturbations in the different years studied, the results were expressed in percentages to avoid misinterpretations that could have resulted from uneven data distribution. The percentages of days with a particular range of TEC perturbations were calculated using the equation

$$\text{Percent. of days} = \frac{N_t}{\text{Ty}_d} \times 100\%, \tag{4}$$

where N_t is the number of days with TEC perturbation in a particular interval (e.g., $2 \leqslant \Delta\text{TEC} < 4$) at a given bin time, and Ty_d is the total number of days in a year with data. The results shown in Fig. 2 reveal that TEC perturbations at EBBE are similar to those at MBAR, with TEC perturbations in the ranges 2–4 TECU being most prevalent with an even distribution between 09:00 LT and 00:00 LT. TEC perturbations in the range 4–6 TECU are less likely than those in the range 2–4 TECU but also have an even distribution between 09:00 LT and 00:00 LT for all the four years considered. Larger amplitude TEC

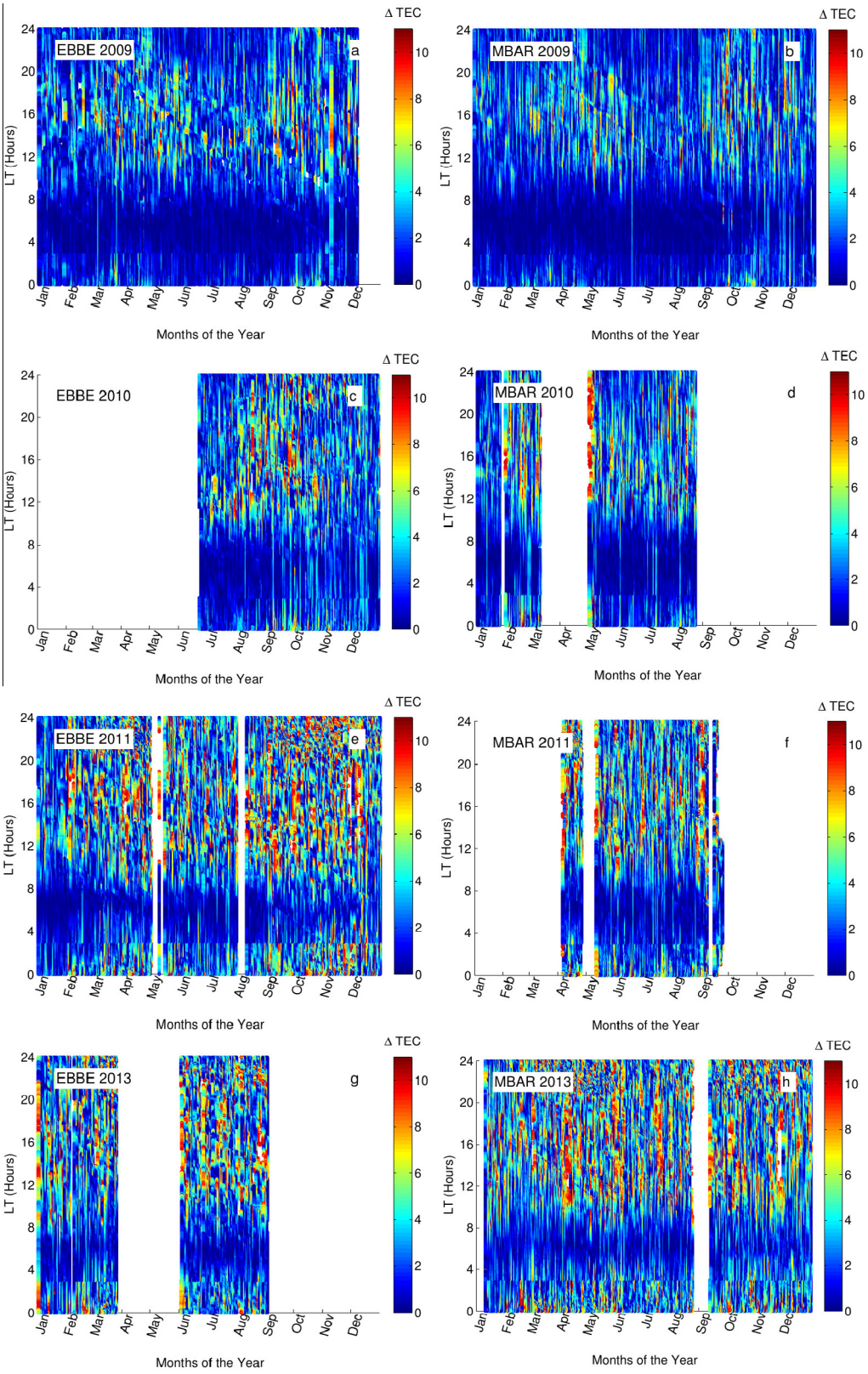

Fig. 1. 30 s absolute TEC perturbations from the monthly medians observed at EBBE and MBAR in 2009, 2010, 2011 and 2013. The approximately zero TEC perturbations from about 03:00–06:00 LT are because the GPS_TEC software forces the vTEC values related to all the visible satellites in this period to be the same in order to estimate the receiver differential bias of each of the GPS satellites.

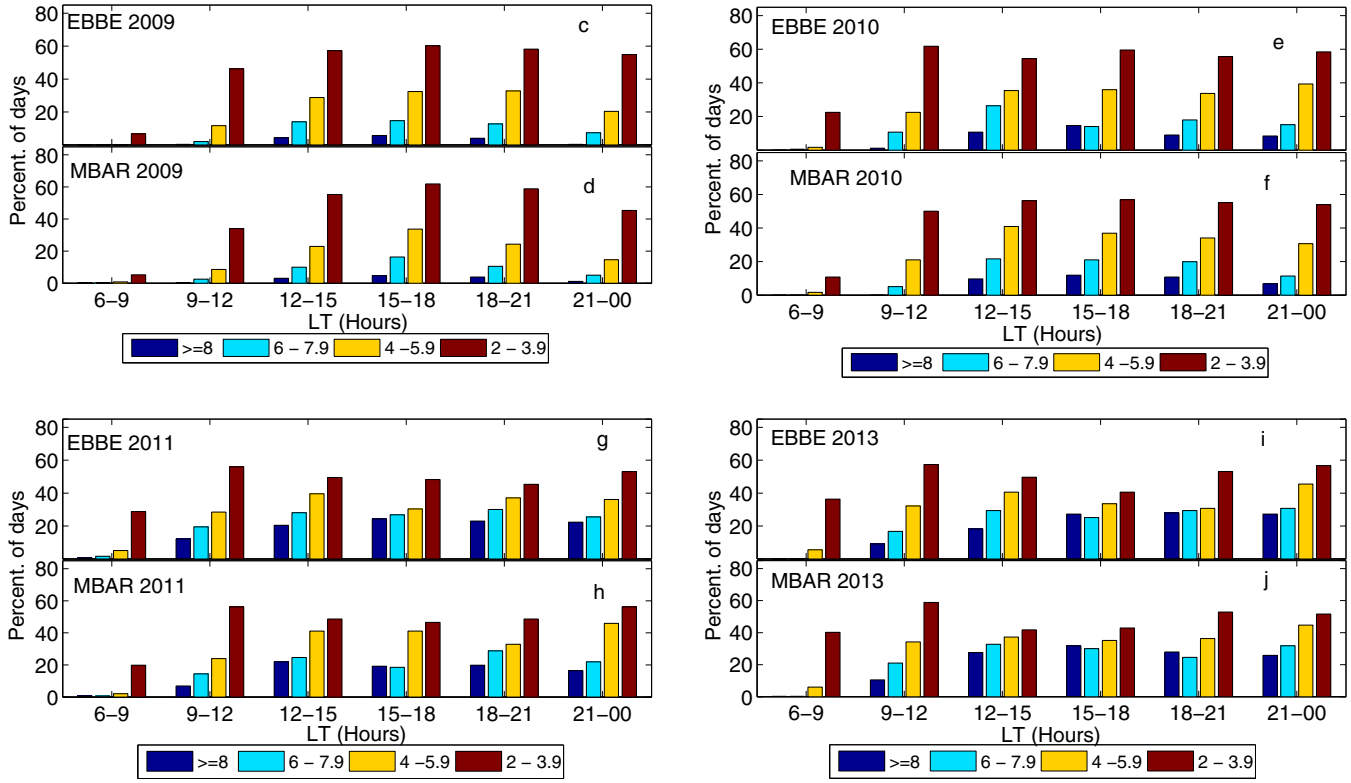

Fig. 2. Diurnal variation of TEC perturbations at EBBE and MBAR in 2009, 2010, 2011 and 2013.

perturbations (ΔTEC ⩾ 8TECU) were observed more frequently from 12:00 to 18:00 LT at both MBAR and EBBE for all the years studied. The probability of ΔTEC exceeding 6 TECU was observed to increase from 2009 to 2013. The high diurnal TEC perturbations from 12:00 to 18:00 LT (Fig. 2) could partly be due to increased perturbations in Extreme Ultra Violet (EUV) radiation (Rishbeth, 1993) associated with 2013 being closer to the solar maximum than 2009. The changes in EUV may cause variations in background temperatures, neutral gas composition and wind speeds, and these in turn modify ionospheric electron density. The increased TEC perturbations observed from 18:00 to 00:00 LT (Fig. 2) could be due to pressure gradient forces that drive neutral wind currents across the solar terminator. Absence of sunlight on the dusk side leads to rapid recombination rates at the bottom of the F layer, creating favorable conditions for generation of plasma irregularities which may be manifested in the TEC perturbations.

3.1.2. Seasonal variation of TEC perturbations

To study the seasonal variation of TEC perturbations, the years under study were divided into seasons as equinoxes (March and September) and solstices (June and December). As noted above, the hourly average TEC perturbations were used to determine the percentages shown in Fig. 3. The probabilities were calculated using the formula

$$\text{Percent. of days of the month} = \frac{N_d}{\text{TN}_d} \times 100\%, \qquad (5)$$

where N_d is the number of days with TEC perturbation in a given range and TN_d is the total number of days with data in the month. TEC perturbations in the range 2–4 TECU occurred almost 100% of the time when data were available at EBBE from 2009 to 2013 and TEC perturbations in the range 4–6 TECU occurred almost 100% of the time when data were available at EBBE in 2011 and 2013, and at MBAR in 2013. TEC perturbations of larger amplitude (6–7.9 & ⩾ 8 TECU) exhibited a clear seasonal pattern (see Fig. 3), with the likelihood of TEC perturbations exceeding 6 TECU being higher during the equinoxes than during the solstices in most years. The exceptions were in the case of EBBE in 2013 where the occurrence of perturbations in the range 6–8 TECU was more likely in Jun than in Mar, and in the case of MBAR in 2013 where the occurrence of perturbations in the range 6–8 TECU was equally likely in Mar and Dec. The Sep equinox had higher probabilities for TEC perturbations in the range 4–6 TECU than the Mar equinox at EBBE in 2011 and at MBAR in 2013. The pattern was reversed in other years, i.e. in 2009 the Mar equinox at EBBE had higher probability for TEC perturbations in the range 4–6 TECU at both EBBE and MBAR in 2011, and in 2013 the Mar equinox showed higher probability for TEC perturbations >8 TECU than the Sep equinox at MBAR. There was no consistent pattern of seasonal dominance of TEC perturbations for the period investigated, which is expected for equatorial stations where there are no marked differences between the seasons as in higher latitudes. In the cases where there

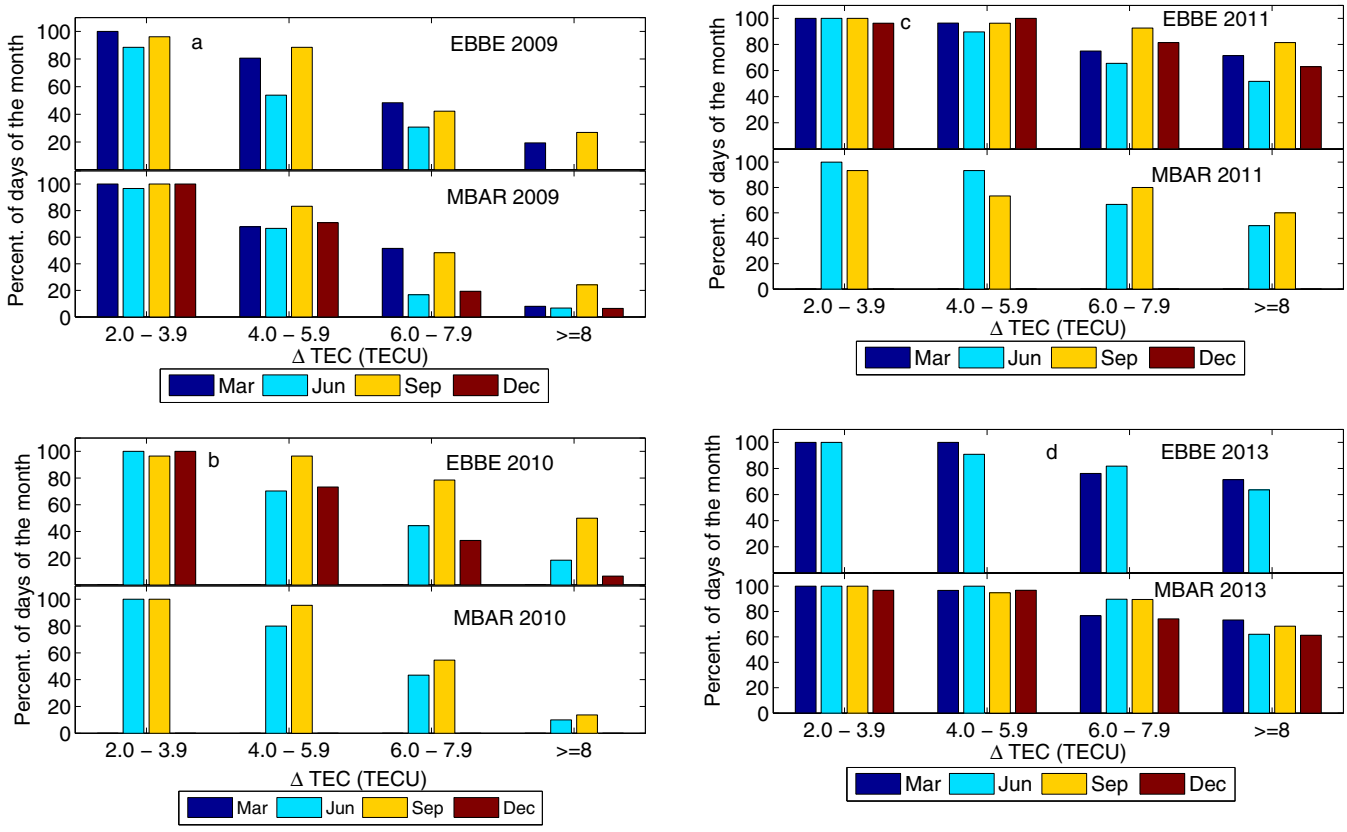

Fig. 3. Seasonal variation of the TEC perturbations in 2009, 2010, 2011 and 2013.

was a higher incidence of large perturbations during the equinoxes than during the solstices, the following explanation may be valid. The nearly 90° solar elevation angle during the equinoctial months may lead to increased solar flux induced variations in the chemical composition, background temperatures and ionospheric conductivities. Under the influence of the enhanced ionospheric conductivities and temperatures during the equinoxes, electrodynamic processes at the equator are enhanced in the equinoctial months resulting in the higher perturbations observed during equinoxes.

3.1.3. TEC perturbations and F10.7

The ionosphere is known to be primarily driven by solar radiation. The sunspot number (SSN) and F10.7 are commonly used solar proxies to indicate the level of solar activity. To compare TEC perturbations with solar activity, F10.7 data obtained from www.spidr.ngdc.noaa were used. Daily maximum and minimum values of hourly mean TEC deviations were calculated and then compared with the daily values of F10.7. Fig. 4 shows the results for 2009, 2011 and 2013 at MBAR while in Table 2, the correlation coefficients at MBAR and EBBE for all the years studied are presented.

Both TEC enhancements and TEC depletions show a weak positive correlation with F10.7. A higher correlation was obtained between F10.7 and TEC enhancement, than between F10.7 and TEC depletion, with a maximum coefficient ($R = 0.322$) in 2013 at MBAR followed by $R = 0.320$ in 2011 at EBBE. The correlation coefficients of F10.7 and TEC depletions were also observed to generally increase from 2009 to 2013 (Fig. 4).

However, anomalous anti correlation was observed between F10.7 and TEC depletions at EBBE in 2011. This negative correlation could be purely statistical or due to other factors. The weak correlation between TEC perturbations and F10.7 are similar to results of Liu et al. (2012), who found a weak positive correlation between F10.7 and daily peak vTEC during a low solar activity period. However, Galav et al. (2010) found good correlation between TEC and F10.7 during the declining phase of solar activity. They argued that solar flux is the dominant parameter to which ionospheric variation in the daytime TEC could be attributed.

3.2. Wave-like structures

Wave-like variations in critical frequency of F2 layer (foF2) and the maximum virtual height of F layer (h′F) are common features during quiet conditions (Klausner et al., 2009). The low latitude ionosphere is characterized by a number of irregularities which make it quite a challenge in studying wave-like variations in TEC perturbations such as those caused by TID. In our multi-filtering techniques, GPS TEC data at MBAR from 2009 to 2013 were analyzed. Wavelet power spectrum, often called

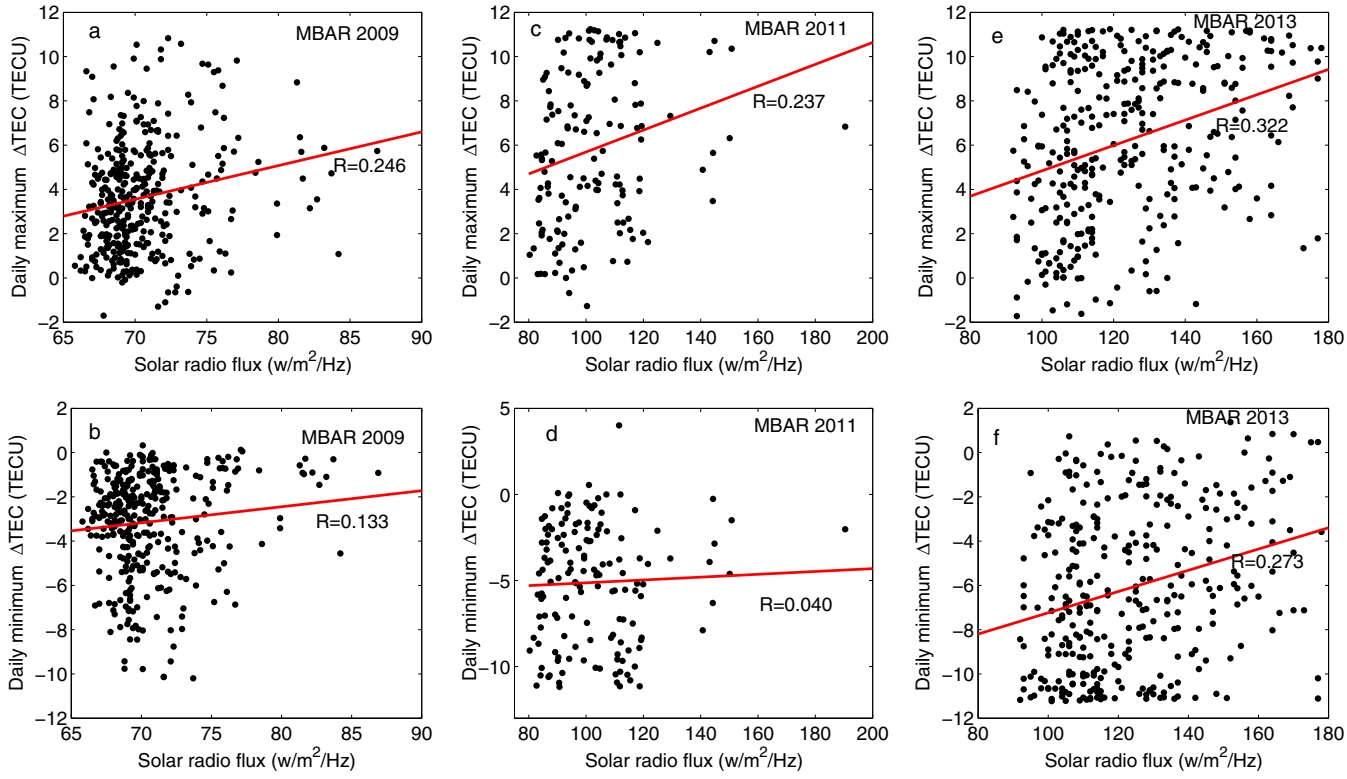

Fig. 4. Comparison of F10.7 with daily maximum and minimum TEC perturbations. R is the Pearson linear correlation coefficient.

Table 2
Correlation coefficients for F10.7 with TEC perturbations at EBBE and MBAR in 2009, 2010, 2011 and 2013.

	R for TEC enhancement				R for TEC depletions			
	2009	2010	2011	2013	2009	2010	2011	2013
EBBE	0.254	0.181	0.320	0.256	0.060	0.145	−0.132	0.277
MBAR	0.246	0.259	0.237	0.322	0.133	0.238	0.040	0.273

scalograms were computed for the entire length of the signal. Signals with spectral components at a particular wavelet scale give relatively larger values of the wavelet power at that particular scale and position. The period and the time of occurrence of the WLS were then read from the scalograms. Using only TID periods as a parameter, we classified the WLS into large and medium scale WLS corresponding to the periods of LSTID (1–3 h) and MSTID (15–60 min) respectively. Fig. 5 shows some of the scalograms for the WLS observed in the TEC perturbations with periods typical of TID. Fig. 5(c) shows that a Large Scale WLS (LSWLS) with period ranging from 100 to 120 min were observed at MBAR from 13:00 to 18:00 LT on Day Of the Year (DOY) 130 in 2010. A similar LSWLS of period 110–120 min were also observed from 13:00 to 23:00 LT on DOY 127 in 2013 at MBAR (Fig. 5 (d)). Medium Scale WLS (MSWLS) of period ranging from 30 to 45 min were observed at MBAR on DOY 107 in 2009 from 22:00 to 00:00 LT (Fig. 5(a)). The data for the occurrence of the WLS were collected and then used for the diurnal and seasonal analysis.

3.2.1. Diurnal variation of wave-like structures

To investigate the diurnal changes in the occurrence of the WLS, a day was divided into four 6-h periods namely morning (07:00–13:00 LT), afternoon (13:00–19:00 LT), evening (19:00–01:00 LT) and night (01:00–07:00 LT). The probabilities shown in Fig. 6 were arrived at by expressing the number of WLS in a given observational interval as a ratio of the number of days with data in the year. This was to give a better comparison of the occurrence of these WLS over the years since the number of days analyzed were uneven for the years studied.

Fig. 6 shows that the probability of occurrence of WLS increased from 2009 to 2013 for both MSWLS and LSWLS. The WLS had higher probability of occurrence between 13:00 and 19:00 LT for 2009–2011, with maximum probability of 0.08 for MSWLS, and 0.02 for LSWLS in 2011 (Fig. 6(c)). However in 2013, both MSWLS and LSWLS had higher probability of occurrence from 19:00 to 01:00 LT (Fig. 6(d)). The probability of occurrence of LSWLS were least from 01:00 to 07:00 LT in all the years studied. Similarly MSWLS had the least probability of

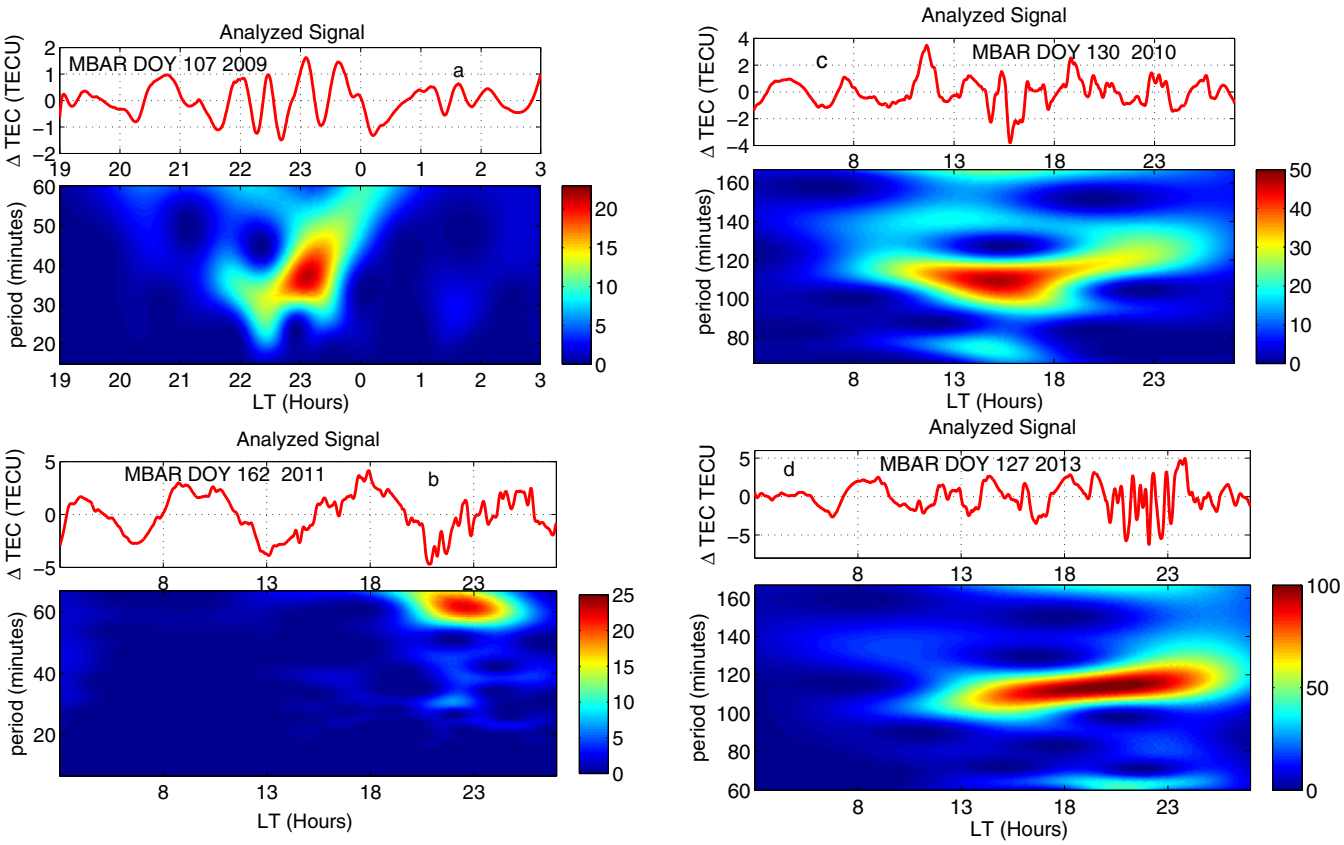

Fig. 5. Scalograms of ΔTEC on 17 April 2009 (a), 11 June 2011 (b), 10 May 2010 (c) and 07 May 2013 (d).

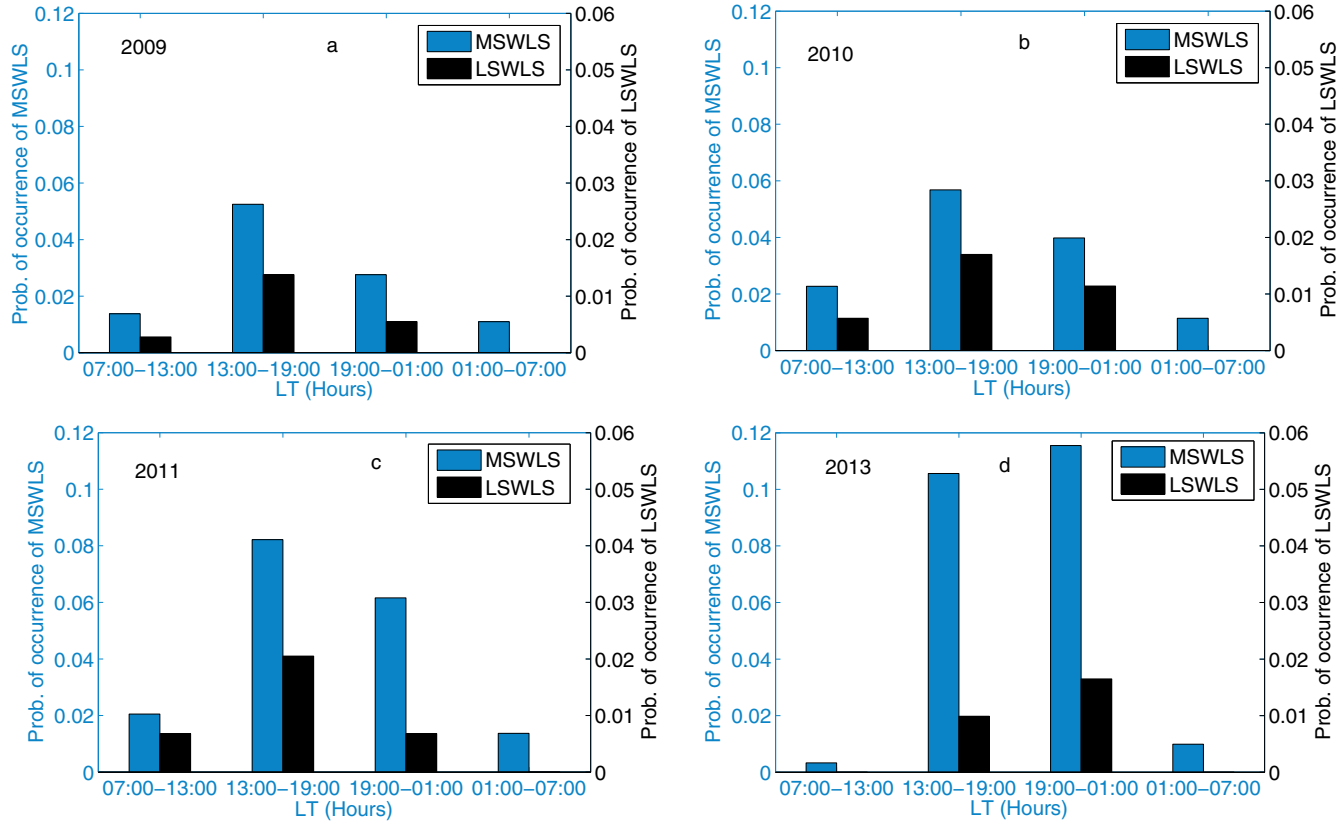

Fig. 6. Diurnal variation of wave-like structures in (a) 2009, (b) 2010, (c) 2011 and 2013 (d).

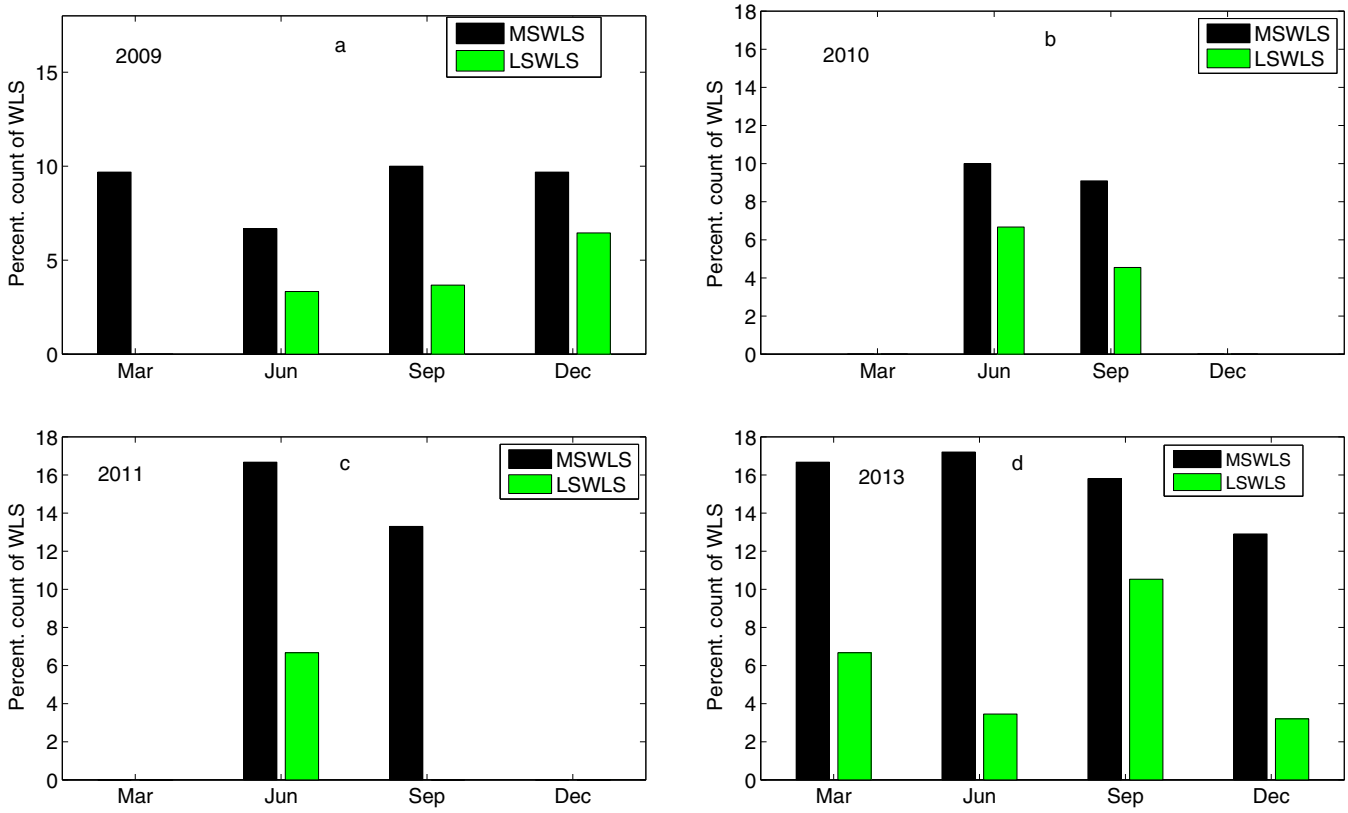

Fig. 7. Seasonal variation of the wave-like structures in 2009 (a), 2010 (b), 2011 (c) and 2013 (d).

occurrence from 01:00 to 07:00 LT except in 2013, where the least probability was observed from 07:00 to 13:00 LT (Fig. 6(d)). The diurnal pattern depicted in this result could be due to variations in viscosity and thermal coefficients resulting from changes in atmospheric temperature with solar radiation, especially if these WLS were induced by GW that originated from the lower atmosphere (Vadas and Fritts, 2004). A study by Vadas and Liu (2009) showed that when the thermosphere is hotter, GW dissipate at higher altitudes than when the thermosphere is cooler. This may explain the high probability of occurrence of WLS from 13:00 to 19:00 LT (Fig. 6(a)–(c)).

3.2.2. Seasonal variation of wave-like structures

The data for the observed WLS for the months of March, June, September and December were extracted and used to investigate any likely seasonal pattern. The percentages shown were arrived at by expressing the number of WLS obtained in a given season as a percentage of the number of days in the month. Fig. 7 shows that MSWLS appeared more frequently than LSWLS at all times and seasons. Wave activity increased gradually from 2009 to 2013 for both MSWLS and LSWLS. However the observation of no WLS in Mar and Dec in 2010 and 2011 was due to missing data in these seasons. MSWLS showed peak occurrence during Sep equinox in 2009 (Fig. 7(a)), while in the rest of the years studied, the peaks were observed in Jun solstice (Fig. 7(b)–(d)). The percentage of LSWLS was observed to be highest during Sep equinox in 2013 (Fig. 7(d)). On the other hand, the peaks of LSWLS occurred during Jun solstice in 2010 and 2011, and Dec solstice in 2009. Generally, there was no clear seasonal pattern observed. This observation is similar to that of Klausner et al. (2009) during a low solar activity period. Changes in the neutral gas density over the years due to variation in solar radiation could partly account for this observation.

3.3. Conclusion

This study has presented the extent of ionospheric perturbations over a low latitude region using GPS TEC. The findings show that daytime TEC perturbations were generally higher than those at nighttime. The diurnal peak in the TEC perturbations occurred between 12:00 and 18:00 LT. Large amplitude TEC perturbations were more frequent in 2013 than in 2009. A semi-annual variation was observed in the TEC perturbations with peaks during the equinoctial months. In addition, our results show that TEC perturbations have a weak positive correlation with F10.7 for most of the years analyzed. The Anomalous negative correlation coefficient between F10.7 and TEC depletions observed in 2011 (Table 2) could have been purely statistical or due to other factors which need further investigations. This suggests that local ionospheric dynamics over the low latitude region is not only driven by changes in solar activity. Wavelet analysis performed on the TEC

perturbations revealed wave-like oscillations with periods typical of TID. The wave-like oscillations showed high probability of occurrence from 13:00 to 19:00 LT with no seasonal pattern. We suggest that the WLS be investigated further to determine whether they were TID, and how they contributed to the observed TEC perturbations.

Acknowledgement

This work was financed by the International Science Programme (ISP). Part of the work was done at South African National Space Agency (SANSA) Space Science Directorate. The first author is grateful to the administration and staff of SANSA for providing a supportive environment during the study visit. The authors wish to thank Dr. Anguma K. Simon for his contribution towards this study. Further appreciation goes to Mr. Vumile Tyalimpi for his contributions towards the MATLAB scripts used in this study. The GPS data were obtained from www.data-out.unavco.org.

References

Abdu, M.A., Ramkumar, T.K., Batista, I.S., Brum, C.G.M., Takahashi, H., Reinisch, B.W., Sobral, J.H.A., 2006. Planetary wave signatures in the equatorial atmosphere ionosphere system, and mesosphere E and F region coupling. J. Atmos. Sol.-Terr. Phys. 68, 509–522.

Adewale, A.O., Oyeyemi, E.O., Adeloye, A.B., Mitchell, C.N., Rose, J.A. R., Cilliers, P.J., 2012. A study of L-band scintillations and total electron content at an equatorial station, Lagos, Nigeria. Radio Sci. 47, RS2011.

Afraimovich, E.L., Palamartchouk, K.S., Perevalova, N.P., 1998. GPS radio interferometry of travelling ionospheric disturbances. J. Atmos. Sol.-Terr. Phys. 60, 1205–1223.

Amabayo, E.B., Edward, J., Cilliers, P.J., Habarulema, J.B., 2014. Climatology of ionospheric scintillations and TEC trend over the Ugandan region. Adv. Space Res. 53, 734–743.

Balan, N., Bailey, G.J., Abdu, M.A., Oyama, K.I., Richards, P.G., MacDougall, J., Batista, I.S., 1997. Equatorial plasma fountain and its effects over three locations: evidence for an additional layer, the F3 layer. J. Geophys. Res. 102, 2047–2056.

Chen, P.R., 1992. Two-day oscillations of the equatorial ionization anomaly. J. Geophys. Res. 979, 6343–6357.

D'ujanga, F., Baki, P., Olwendo, J., Twinamasiko, B., 2013. Total electron content of the ionosphere at two stations in East Africa during the 24–25 October 2011 geomagnetic storm. Adv. Space Res. 51, 712–721.

Fritts, D.C., Alexander, M.J., 2003. Gravity wave dynamics and effects in the middle atmosphere. Rev. Geophys. 41 (1), 1003.

Galav, P., Dashora, N., Sharma, S., Pandey, R., 2010. Characterization of low latitude GPS-TEC during very low solar activity phase. J. Atmos. Sol.-Terr. Phys. 72, 1309–1317.

Habarulema, J.B., Katamzi, Z.T., McKinnell, L.A., 2013a. Estimating the propagation characteristics of large-scale traveling ionospheric disturbances using ground-based and satellite data. J. Geophys. Res. 118, 7768–7782.

Habarulema, J.B., McKinnell, L.A., Burešovà, D., Zhang, Y., Seemala, G., Ngwira, C., Chum, J., Opperman, B., 2013b. A comparative study of TEC response for the African equatorial and mid-latitudes during storm conditions. J. Atmos. Sol.-Terr. Phys. 102, 105–114.

Hernández-Pajares, M., Juan, J.M., Sanz, J., 2006. Medium-scale traveling ionospheric disturbances affecting GPS measurements: spatial and temporal analysis. J. Geophys. Res. 111, A07S11.

Hunsucker, R.D., 1982. Atmospheric gravity waves generated in the high latitude ionosphere. Rev. Geophys. 20, 293–315.

Katamzi, Z.T., Smith, N.D., Mitchell, C.N., Spalla, P., Materassi, M., 2012. Statistical analysis of traveling ionospheric disturbances using TEC observations from geostationary satellites. J. Atmos. Sol.-Terr. Phys. 74, 64–80.

Klausner, V., Fagundes, P.R., Sahai, Y., Wrasse, C.M., Pillat, V.G., Becker-Guedes, F., 2009. Observations of GW/TID oscillations in the F2 layer at low latitude during high and low solar activity, geomagnetic quiet and disturbed periods. J. Geophys. Res. 114, A02313.

Liu, G., Huang, W., Shen, H., Gong, J., 2012. Vertical TEC variations and model during low solar activity at a low latitude station. Xiamen. Adv. Space Res. 49, 530–538.

Luo, J., Ying, K., He, P., Bai, J., 2005. Properties of Savitzky–Golay digital differentiators. Digital Signal Process. 15, 122–136.

MacDougall, J., Abdu, M., Batista, I., Fagundes, P., Sahai, Y., Jayachandran, P., 2013. On the production of traveling ionospheric disturbances by atmospheric gravity waves. J. Atmos. Sol.-Terr. Phys. 71, 2013–2016.

Martyn, D.F., 1947. Atmospheric tides in the ionosphere, I. Solar tides in the F2 region. Proc. R. Soc. Lond. 189, 241–260.

Mendillo, M., 2006. Storms in the ionosphere: patterns and processes for total electron content. Rev. Geophys. 44, RG4001.

Misiti M., 2005. Wavelet Toolbox: For Use with MATLAB: User's Guide. MathWorks Inc.

Olwendo, O., Baki, P., Mito, C., Doherty, P., 2012a. Characterization of ionospheric GPS total electron content (GPS-TEC) in low latitude zone over the Kenyan region during a very low solar activity phase. J. Atmos. Sol.-Terr. Phys. 84–85 (2012), 52–61.

Olwendo, O., Cilliers, P., Baki, P., Mito, C., 2012b. Using GPS-SCINDA observations to study the correlation between scintillation, total electron content enhancement and depletions over the Kenyan region. Adv. Space Res. 49, 1363–1372.

Rishbeth, H., 1993. Day-to-day variations in a period of high solar activity. J. Atmos. Sol.-Terr. Phys. 55 (165–171), 1993.

Seemala, G.K., Valladares, C., 2011. Statistics of total electron content depletions observed over the South American continent for the year. Radio Sci. 46, RS5019.

Vadas, S.L., Fritts, D.C., 2004. Thermospheric responses to gravity waves arising from mesoscale convective complexes. J. Atmos. Sol.-Terr. Phys. 66, 781–804.

Vadas, S.L., Liu, H., 2009. Generation of large scale gravity waves and neutral winds in the thermosphere from the dissipation of convectively generated gravity waves. J. Geophys. Res. 114, A10310.

Further reading

Amabayo, E.B., McKinnell, L.A., Cilliers, P.J., 2011. Statistical characterisation of spread F over South Africa. Adv. Space Res. 48, 2043–2052.